

# Evaluation of Fracture Strength and Material Degradation for Weldment of High Temperature Service Steel Using Advanced Small Punch Test

**Dong-Hwan Lee\***

*Division of Mechanical & Aerospace System Engineering, Chonbuk National University,  
Chonju, Chonbuk 561-756, Korea*

This paper presents an effective and reliable evaluation method for fracture strength and material degradation of the micro-structure of high temperature service steel weldment using advanced small punch (ASP) test developed from conventional small punch (CSP) test. For the purpose of the ASP test, a lower die with a minimized  $\Phi 1.5$  mm diameter loading ball and an optimized deformation guide hole of  $\Phi 3$  mm diameter were designed. The behaviors of fracture energy ( $E_{sp}$ ), ductile-brittle transition temperature (DBTT) and material degradation from the ASP test showed a definite dependency on the micro-structure of weldment. Results obtained from ASP test were compared and reviewed with results from CSP test, Charpy impact test, and hardness test. The utility and reliability of the proposed ASP test were verified by investigating fracture strength, behavior of DBTT, and fracture location of each micro-structure of steel weldment for test specimen in ASP test. It was observed that the fracture toughness in the micro-structure of FL+CGHAZ and ICHAZ decreased remarkably with increasing aging time. From studies of all micro-structures, it was observed that FGHAZ microstructure has the most excellent fracture toughness, and it showed absence of material degradation.

**Key Words:** Advanced Small Punch (ASP) Test, Conventional Small Punch (CSP) Test, Material Degradation, Heat Affected Zone (HAZ), Ductile-Brittle Transition Temperature (DBTT)

## 1. Introduction

Material degradation caused by long term operation hysteresis under high temperature and pressure is an important issue and is closely related to assuring the safety and life-time extension of Power Plant facilities. In case material degradation occurs at weldment of an engineering structure which has a fundamental weakness, existing test methods like the Charpy v-notch (hereinafter referred as CVN) test becomes delimited in its

application for evaluation due to the complexity and localization of the particular structure of weldment.

Various kinds of non-destructive tests have been actively applied to overcome the limitations of the traditional destructive test method (Nishiyama, 1998; Haggag, 1998; Kim, 1991). However, the evaluation results obtained from these non-destructive test are unreliable because the results do not agree with results from destructive test. Thus, it is necessary to achieve a correlation between the destructive and non-destructive test. Furthermore, it is necessary to obtain a suitable evaluation technique for material degradation to overcome the problems caused by the application of these test methods.

Generally, various and complicated micro-

---

\* E-mail : hsb9020@unitel.co.kr

TEL : +82-63-270-2346; FAX : +82-63-270-2460

Division of Mechanical & Aerospace System Engineering, Chonbuk National University, Chonju, Chonbuk 561-756, Korea. (Manuscript Received March 20, 2004;

Revised July 19, 2004)

structures are produced by the multiple path welding of steel plate and pipe for high temperature service (such as weld metal (WM) and heat affected zone (HAZ)). In addition, there are more complicated regions in the HAZ (e.g coarse grain region (CGHAZ), fine grain region (FGHAZ), inter-critical grain region (ICHAZ), and tempered grain region (TGHAZ)) that will be generated in the final path on the weld preparation. These regions have microstructures and the distances between each micro-structure are very limited. These regions of HAZ are created near the fusion line (FL) and have different microstructures with different mechanical properties. Also, they have lower values of strength, lower fracture toughness and are largely affected by the fracture of weldment (Chung, 1978; Viswanathan, 1993) compared to the base metal (BM).

The small punch (SP) test (Baik, 1986; Lyu, 1989; Yu, 1998) and continuous indentation test (Haggag, 1998) have been developed and applied to evaluate mechanical properties of the micro-structure in steel weldment. Basically, the evaluation of characteristics for the micro-structure of weldment shows a limitation through the SP test i.e. SP test is generally applied by  $\phi 2.4$  mm steel ball as a loading ball but, if a deformation region applied by the steel ball surpasses its own individual region (for each HAZ), the SP test becomes limited. Therefore, the application of a

micro-steel ball and precise jig will be required, thus guaranteeing the possibility of a precise evaluation for the micro-structure of steel weldment.

Consequently, with respect to the virgin material and aged material of high temperature service steel for the power plant, this study investigated the possibility of evaluating the fracture strength and material degradation at regions of steel weldment by introducing an advanced small punch (ASP) test which is developed from conventional small punch (CSP). Results obtained by the ASP test for various weldment structures were investigated to verify its (ASP test) availability and reliability. The results were compared with results of CSP test, CVN impact tests, and hardness test.

## 2. Test Materials and Methods

### 2.1 Test materials

The material used in this study is X20CrMoV121 steel, and the chemical compositions and mechanical properties at room temperature are shown in Table 1 and 2 respectively. The welding procedures and conditions applied in the actual power plant were used, and shown in Table 3 and 4.

In addition, the isothermal aging heat treatment for specimen was performed in order to investigate the behavior of material degradation

**Table 1** Chemical composition of X20CrMoV121 steel (wt%)

C	Si	Mn	P	S	Ni	Cr	Mo	V	Fe
0.19	0.19	0.48	0.011	0.003	0.66	10.40	0.86	0.26	bal.

**Table 2** Mechanical properties of X20CrMoV121 steel

Yield strength (MPa)	Tensile strength (MPa)	Elongation (%)	Y/T ratio (%)
572	798	19.4	72

**Table 3** Welding procedure specification for X20CrMoV121 steel

Process (pass)	Filler Metal		Polarity/Current		Voltage Range (V)	Travel speed (cm/min)
	DIN class	Diameter	Type	Amp. range		
GTAW (1~3)	SGCrMoWV12	$\phi 2.4$	DCSP	130~150	11	8~15
SAW (4~34)	UPS2CrMoWV12	$\phi 2.4$	DCSP	305~345	31~32	40~50

**Table 4** Strengthening heat treatment, preheat and PWHT condition for X20CrMoV121 steel

Normalizing	1050°C, 15 min, AC
Tempering	760°C, 90 min, AC
Preheat	120°C, 2 hr 20 min
PWHT	750°C, 5 hr 51 min

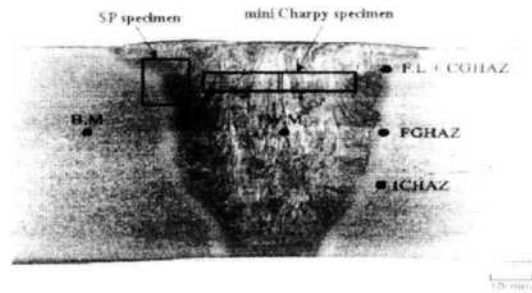
**Table 5** Accelerated aging time

Simulation time in-service at 566°C	Aging time at 660°C
100,000 hrs	2,000 hrs
300,000 hrs	6,000 hrs

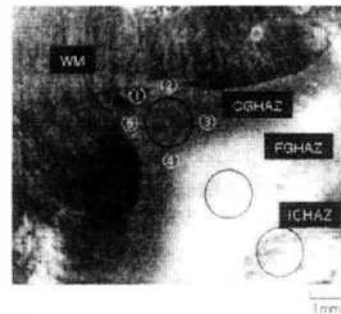
for the test material. A mock-up aging time was decided on the basis of activation energy required for the self diffusion of steel (Abel-Latif, 1981) and was considered for the operating and tempering temperature of the material. Table 5 shows accelerated aging time and isothermal aging heat treatment conditions.

## 2.2 Observation of micro-structures of weldment and preparation of a SP test specimen

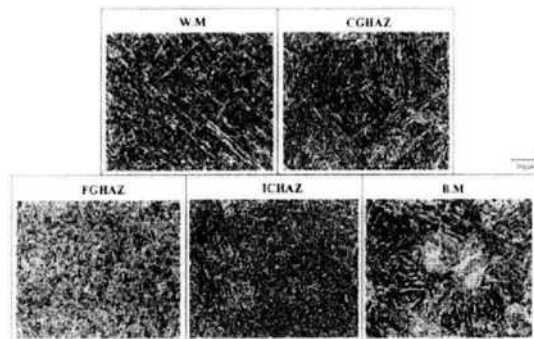
Figure 1 shows a macro-etched structure of weldment for X20CrMoV121 steel. Figure 1(a) shows the machining position for SP and Charpy specimen and Fig. 1(b) shows the magnification view of toe HAZ. SP test specimens, 10 mm × 10 mm × 0.5 mm, were taken from the block-cut-off weldment, and the locations are named ① FL+CGHAZ, ② FGHAZ, ③ ICHAZ, ④ WM, ⑤ BM structure. As shown in Fig. 1(a), SP specimens for each microstructure were cut as each microstructure was placed on the center of specimen. It is expected that the characteristics of the micro-structure of test specimen can be evaluated easily because the open space of loading steel ball is precisely located for each. Each micro-structure of steel weldment has its clear region from FL. As shown in Fig. 2, the observations of the micro-structures show that the BM is a lath martensite structure and the region of HAZ is constructed with CGHAZ of coarse grain, FGHAZ of fine grain, and ICHAZ mixed with BM and FGHAZ. In the region of WM,



(a) Machining position and direction



(b) Magnification view of toe HAZ

**Fig. 1** Macro-etched structure of weldment**Fig. 2** Micro-structures of virgin weldment

there is a mixed structure where some parts of structure are particularized at the overlapped region due to the tempering effect of the preceding and escorting path. Some of the particularized structure at the overlapped region mixed with the columnar static structure of coarsening structure.

## 2.3 SP test and CVN impact test

After considering the size of deformation guide hole (DGH) that is machined at the lower die of the ASP test jig, an optimal jig design can

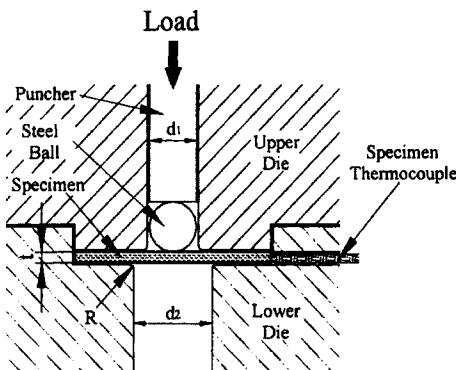
be determined to apply for the micro-structure of steel weldment (Lee, 2002). Results obtained showed an effect on test specimen thickness.

Figure 3 shows the diagram for SP test jig, and Table 6 shows the major specifications of the CSP and ASP test jig.

A behavior of load-displacement is measured in the SP test, and the SP energy  $E_{SP}$  ( $E_{CSP}$  for CSP and  $E_{ASP}$  for ASP) can be measured by the area located below the curve. Ductile-brittle transition temperature (DBTT) can also be obtained by the temperature dependent curves of ESP for each structure using the temperature range from  $-196^{\circ}\text{C}$  to room temperature (R.T). For this cryogenic test environment, the SP and CVN test were performed in liquid nitrogen environment. And, the DBTT is defined as the application temperature of the upper and lower average values of ESP. Detailed methods and procedures on the SP test are based on the results of a former study (Lyu, 1989; Yu, 1998). To ensure reliability, a CVN impact test was carried out and compared with qualitative analysis results of SP test.

**Table 6** Dimensional comparison for CSP and ASP test jig (unit : mm)

Item	CSP	ASP
Puncher diameter, $d_1$	2.4	1.5
Steel ball diameter	2.4	1.5
DGH diameter, $d_2$	4.0	3.0
Specimen thickness, $t$	0.5	0.5
Curvature radius, $R$	0.2	0.2



**Fig. 3** The schematic diagram of SP test jig

The test was performed by a 357.9 J impact tester from Tinius Olsen, and the test specimens were made with  $2.5\text{ mm} \times 10\text{ mm} \times 55\text{ mm}$  of sub-size (based on ASTM E 23-93a) that has a notch radius of 0.25 mm, depth of 2 mm, and an angle of  $45^{\circ}$ . The CVN impact test was only applied to the BM and WM structure as it is considered a totally limited weldment characteristics of the structure.

### 3. Results and Discussions

#### 3.1 Hardness distribution of micro-structure for steel weldment

The micro-Vicker's hardness distribution in micro-structure according to aging heat treatment for weldment is illustrated in Fig. 4. In case of virgin material weldment, the distribution of hardness from the CGHAZ and WM adjacent to the FL is shown to be about 300~330 and highly distributed compared with the BM. From Fig. 4, a weakened layer which will undergo temperature range from  $A_{c1}$  to  $A_{c3}$  transformation temperature for welding, and which has a lower hardness than that of BM (at the region of ICHAZ) can be observed.

The aged materials for 2000 hours and 6000 hours present a lower hardness than the virgin material, but is slightly increased for 6000 hours. It is assumed that a weakening behavior due to

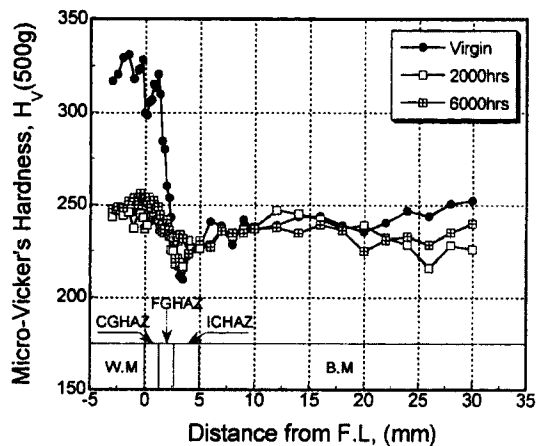


**Fig. 4** Micro-hardness distributions in steel weldment

the spheroid and coarsening of carbon as a typical material degradation occurs. Consequently, a sudden decrement of hardness is shown at the region of CGHAZ and WM relatively implying that the structures are very sensitive to the weakening caused by material degradation. Furthermore, the weakened layer can be found in the ICHAZ structure of an aged material.

### 3.2 Characteristics of SP fracture for micro-structure of steel weldment

Figure 5 presents the comparison between the  $E_{SP}$  calculated by load-displacement curve at room temperature for each structure of HAZ, BM and WM and the results of ASP and CSP tests. The value of  $E_{SP}$  is an important physical quantity because it represents the loading capacity and fracture characteristics of the material in the SP test.

A fine structure of FGHAZ shows the biggest values of ESP, but the coarsening structure of FL+CGHAZ and WM, (which is a kind of melting and solidification structure) present the lowest values. Generally, it showed a dependency for the region of HAZ structure similar to that of the CSP test regardless of the values of ESP in the ASP test (i.e. a small steel ball, and much smaller diameter of DGH compared to that of the CSP test).

A behavior of load-displacement obtained by the ASP test at  $-196^{\circ}\text{C} \sim$  room temperature for the FL+CGHAZ structure known as the most remarkable region of the degradation of fracture toughness for the micro-structure of weldment is shown in Fig. 6.

This implies that the load-displacement curve moves from a low temperature region to a high load side due to the effect of the increment of yield strength caused by the decrement of the application temperature (Abel-Latif, 1981). Additionally, it shows a behavior of brittleness with a sudden decrement of load (after the maximum load at the low temperature region under  $-160^{\circ}\text{C}$ ) and a behavior of ductility with a gentle decrement of load (after the maximum load according to the increment of temperature over  $-120^{\circ}\text{C}$ ).

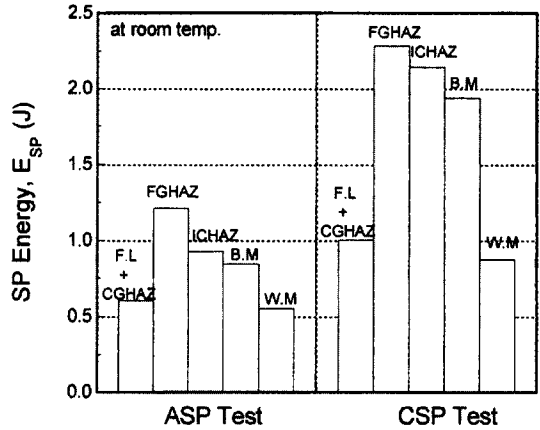


Fig. 5 A comparison of ESP from various micro-structures at R.T in SP test

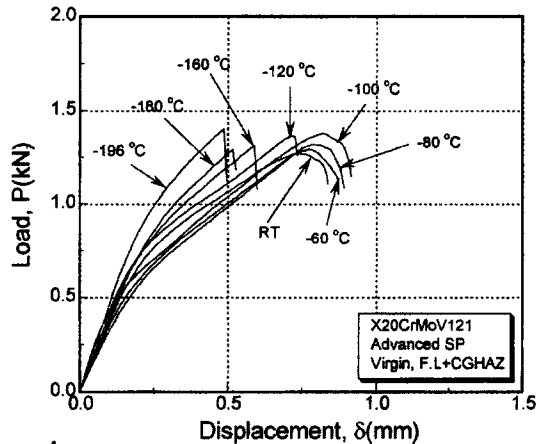


Fig. 6 The load-displacement curves obtained from FL +CGHAZ at various temperatures in ASP test

### 3.3 Ductile-brittle transition and a behavior of degradation for the welding structure

#### 3.3.1 Results of the CVN impact test

A behavior of the CVN impact absorption energy for the application temperature of WM structure is presented in Fig. 7. Generally, the transition curves of aged material are located at the low temperature side (compared with virgin material), but for 6000 hrs, it moves to the high temperature side. Figure 8 presents a material degradation which is defined as the differences of DBTT between the virgin material of WM and

BM, the individual aged materials (whose DBTT can be obtained by the behavior of transition), and  $\Delta(\text{DBTT})_{\text{CVN}}$  together with the characteristics of hardness.

Two structures show the decrement of  $\Delta(\text{DBTT})_{\text{CVN}}$  at 2000 hours that is applicable to  $566^\circ\text{C}/100,000$  hours, and is apt to increase at 6000 hours which is applicable to  $566^\circ\text{C}/300,000$  hours.

As shown, the material degradation is increased at a condition of 6000 hours as compared with the BM structure. Nonetheless, the WM structure still shows an improved fracture toughness in spite of increment in material degradation. The affecting of long term aging heat treatment is to be released

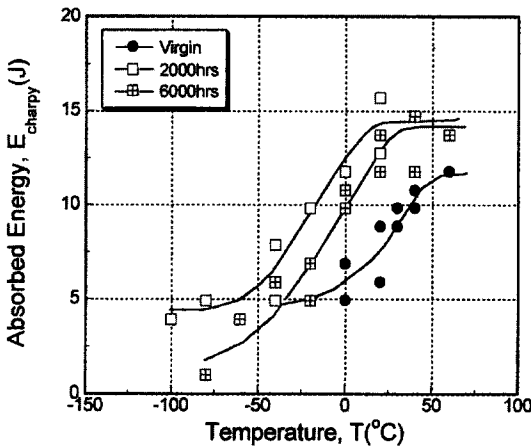


Fig. 7 CVN impact absorbed energy of WM

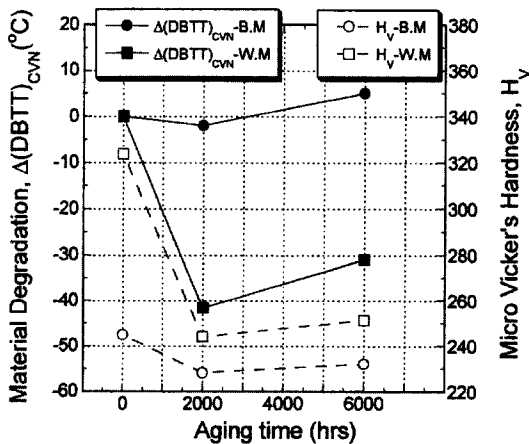
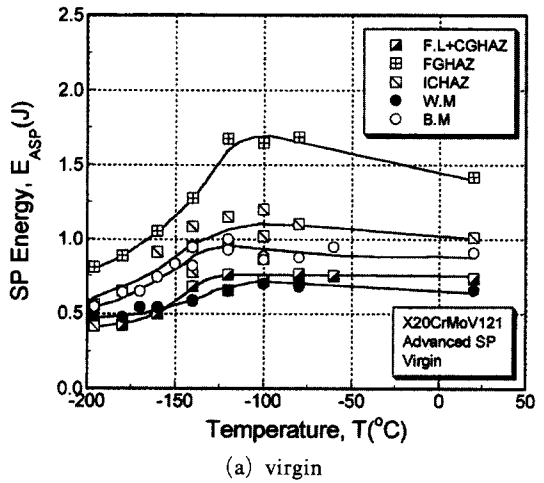


Fig. 8 Variation of  $\Delta(\text{DBTT})_{\text{CVN}}$  and micro Vicker's hardness

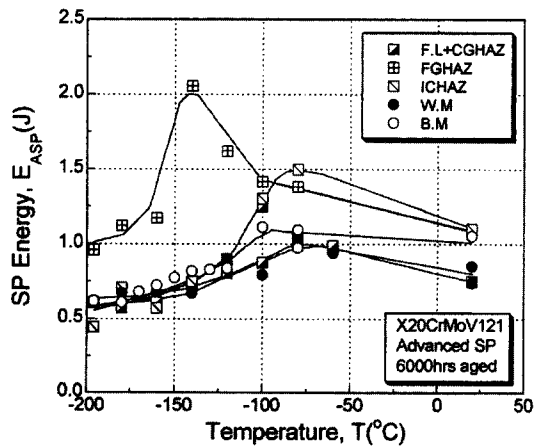
the residual stress generated during welding process. However, the changes of  $\Delta(\text{DBTT})_{\text{CVN}}$  for two structures are nearly the same as the changes of hardness. Thus, a behavior of material degradation can be expected by means of a non-destructive method through the characteristics of hardness.

### 3.3.2 Results of CSP and ASP test

Figure 9 shows the values of EASP of the virgin and 6000 hrs aged material for the BM, WM and HAZ structures with respect to the test temperature. The SP energy of 6000 hrs aged material is slightly increased compare to that of



(a) virgin



(b) 6000 hrs

Fig. 9 SP energy transition behaviors for various micro-structures of virgin (a) and 6000 hrs aged material (b) in ASP test

virgin material. The affecting of long term aging heat treatment is to be released the residual stress, and stress constraint and heat treatment generated during welding process. This behavior can be also verified in SEM (scanning electron microscope) microstructure of Fig. 10. As shown in the figure, the carbide in virgin material is distributed over the structure, but in 6000 hrs aged material, the carbide of each structure is concentrated on the boundary of lath phase. So, it is thought that the SP energy is increased as increasing aging time due to this carbide behavior, as well as the release of residual stress and stress constraint.

However, The differences in the transition behaviors of EASP in the HAZ structures that are continued and arranged between BM and WM structure is clearly shown in the Fig. 9. So, it can be known that the ASP test method is very useful.

The structure of FGHAZ that has a fine granule was definitely superior to others in terms of strength and ductility. Furthermore, the values of ESP are the highest for the whole application temperatures, and DBTT was located in the lowest temperature side.

Thus, the fracture toughness of the structure of FGHAZ is relatively superior to others when the relative idea of the evaluation of fracture toughness is applied to SP test using FATT (fracture appearance Virgin transition temperature) in the CVN test. Also, it is possible to notice the decrement of relative fracture toughness for the WM and FL+CGHAZ structure as compared with the BM structure. Here, the upper

and lower values of  $E_{SP}$  for the temperature are cleared in all structures, and the temperature dependency of  $E_{SP}$  can be verified in the ASP test. In addition, a behavior of the ductile-brittle transition temperature can be found at the same temperature ranges similar to those of CSP test. Previous studies (Chung, 1978 ; Baik, 1986) have verified that a more accurate evaluation of the DBTT can be performed because the ductile-brittle transition temperature occurs at the more narrow temperature ranges due to the large value of the curvature that moves from the highest values of energy to the lowest values as compared with the CVN impact test.

The  $\Delta(DBTT)_{SP}$  values of the mentioned ASP and CSP tests (for the micro-structure of weldment) are shown in Fig. 11 according to the aging times. The behaviors of the degradation for each structure are clearly different.

First of all, almost all behaviors of degradation for the aging times are almost the same as the results of the CVN impact test, except for the FL+CGHAZ structure in the ASP test. However, in case of the BM and WM, the material degradation has a tendency to increase as compared with the virgin material and the aged material for 6000 hours. Furthermore, degradation of the FL+CGHAZ structure is smoothly increased by the increment of aging times, but the structures of BM, ICHAZ, and WM show decrement of degradation for the condition of 2000 hours as compared with the virgin material. Nevertheless, it presents an increment of degradation at the condition of 6000 hours.



Fig. 10 Microstructures of X20CrMoV121 steel weldment by SEM

There was a definite degradation increase in the ICHAZ structure. However, the FGHAZ structure shows the highest fracture toughness under prolonged aging times compared to other virgin materials including BM and other regions of the HAZ.

The differences in degradation are due to the metallurgical properties according to the conditions of the test method, size of the sample and the welding structure. This means that strength and fracture toughness under the same stress per unit area is decreased as much as the defect increases. Hence, the deformation of the specimen used for the ASP test (that is deformed and destructed around  $\Phi 1.5$  mm of the local area) is more severe compared with the specimen of the CVN impact test. Also, it is sharply sensitive for degradation because there is a high possibility of a large defect according to the progress of degradation. In addition, the distinguished decrement of fracture toughness is considered by the structures

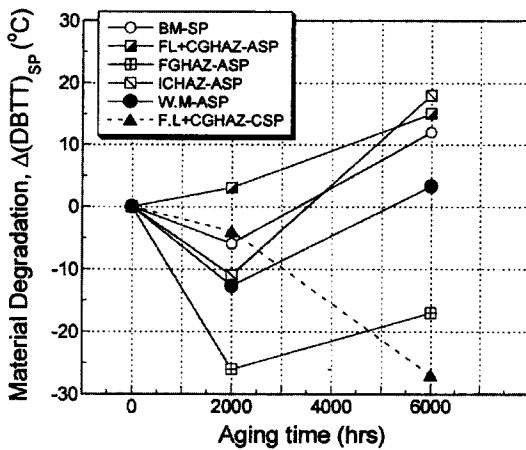


Fig. 11 Variation of D (DBTT)<sub>SP</sub> according to aging times in ASP & CSP test

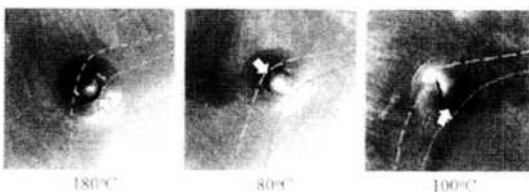


Fig. 12 The fractured position of ASP test for CGHAZ

and is shown in Fig. 4 where the WM and FL + CGHAZ structures show remarkable increment of degradation caused by the aging heat treatment (from results of the hardness test), and the ICHAZ structure that has a local brittleness (Liao, 1998) due to the martensite-austenite (M-A) produced by multi-layered welding.

Figure 11 shows that degradation is slowly increased by the increasing application time in the ASP test (according to the results of FL + CGHAZ). Contrarily, the results of CSP test show a reverse behavior. Therefore, it is impossible to apply these conflicting results in the existing big-test specimen. However, it is possible to verify the failure location of FL + CGHAZ after the SP test through the following macro structure observation.

Figure 12 shows some macro fracture observation obtained from etching the specimen after ASP test. In the figure, the dashed line is fusion line and the dotted line is the boundary between CGHAZ and ICHAZ. As shown in the figure, all fracture position was found in the CGHAZ region. Table 7. presents the fracture ratio according to the result of fracture position after the analysis for the 54 test specimens of FL + CGHAZ. The number ①~⑤ that present the failure locations (directions) are shown in Fig. 1. It shows that the ratio is the same as the CGHAZ structure adjacent to the FL region to the direction of ① and ②, and the CGHAZ structure of the conflict direction ③ and ④ in the ASP test. However, the failures largely occur at the direction of ①, ②, and ⑤ for the FL region in the CSP test owing to the relative increment of the size of the steel ball.

Table 7 Fracture ratio according to failure location in ASP and CSP test specimen (%)

Failure location	ASP	CSP	Remarks
①	13.3	14.3	13.8
②	33.3	42.9	37.9
③	33.3	7.1	20.7
④	13.3	10.7	12.1
⑤	6.6	25.0	15.5



As a result, it is assumed that the failures simultaneously occurred at the various directions in the region of CGHAZ, except for the region of FL because the diameter of the steel ball is definitely small as compared with the width of the CGHAZ region in the ASP test.

Therefore, it is possible to expect that the relative reliability will be ensured from the results of the ASP test (according to the consideration of degradation for other structures for aging times), and from the existence of the region deformed by the steel ball in the micro-structure of the steel weldment (due to the unique and constant failure in the FL+CGHAZ structure for the ASP test). From Table 7, it can be found that the highest ratio of failure occurs at the upper region of FL. The values of  $\Delta(\text{DBTT})_{\text{ASP}}$  for the micro-structure of the weldment obtained by the ASP test according to the aging time with the characteristics of hardness are shown in Fig. 13. Also, it can be found that the changes in values of  $\Delta(\text{DBTT})_{\text{ASP}}$  obtained by the ASP test with changes of hardness, are exactly reflected to the changes of the characteristics of degradation for each welding structure according to aging time. These values of degradation and hardness according to the aging times differ from other structures such as FL+CGHAZ and ICHAZ.

The CGHAZ and FGHAZ structures that are affected by high welding heat were relatively

compared with the ICHAZ structure and they showed a decrease in hardness, i.e. a specific degradation due to aging. However, ICHAZ that is already included with the weakened layer shows an increment in hardness by means of carbon creation, and coarsening due to increment of the aging time even though it is very small. Here, the material degradation of weldment is variously processed by the welding structure. In addition, results of the evaluation of material degradation are limited by the consideration of hardness (because the mechanism is too complicated).

This study investigated the behavior of weldment in view of structure focused on the possibility of applying the ASP test method for micro-structure of weldment, and verifies the possibility of the ASP test for material degradation of weldment. Thus, it is considered that the effects on material degradation of the micro-structure of weldment are caused by the creation of carbon, impurities segregation, M-A (Martensite-Austenite constituent) product of the ICHAZ structure, etc.

#### 4. Conclusions

In conclusion, the possibility of evaluating fracture strength of the micro-structure of weldment and material degradation by introducing the ASP (Advanced Small Punch) test for the virgin material and aged material of X20CrMoV121 steel are summarized as follows:

(1) The absorption energy, ESP and ductile-brittle transition temperature (DBTT) are evaluated for each micro-structure of weldment in the entire process of material failure through the ASP test. The FGHAZ showed the highest values of  $E_{\text{SP}}$ , FL+CGHAZ and WM showed smaller values of  $E_{\text{SP}}$  than BM, implying a clear dependency of the changes of the HAZ structure. Furthermore, DBTT values of FL+CGHAZ, WM, and ICHAZ are located at the side of the high temperature region (compared with FGHAZ). This presents a decrement of relative impact toughness.

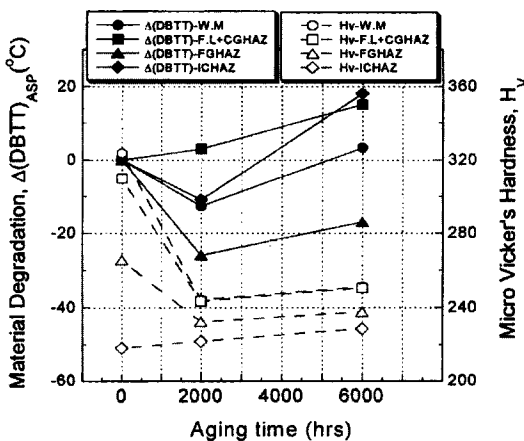


Fig. 13 Relationships between  $\Delta(\text{DBTT})_{\text{ASP}}$  and micro-Vicker's hardness

(2) Material degradations of each micro-structure are changed variously due to the difference of proper metallurgical characteristic. The material degradation of FL+CGHAZ is increased with increasing of aging times. However, the micro-structures of BM, ICHAZ, and WM show a decrease of degradation at the condition of 2000 hours of aging time that is equivalent to 566°C/100,000 hours, and they are degraded remarkably at 6000 hours of aging time that is equivalent to 566°C/300,000 hours. Especially, the increment of material degradation was not presented in FGHAZ structure in spite of increasing aging time, and the highest fracture toughness was showed in FGHAZ structure among the micro-structures of weldment.

(3) FGHAZ has the finest granule among the various micro-structures of weldment and it showed the most excellent values of mechanical properties (such as strength, ductility, fracture toughness, etc.). Also, it showed remarkable ductility in the welding process and aging heat treatment. The WM, FL+CGHAZ, and ICHAZ that present a local brittleness and unevenness showed remarkable decrement of strength and fracture toughness.

(4) Considering the ductile-brittle transition of the weldment for each structure, (from the beginning of degradation and location of failure for the test specimen of the FL+CGHAZ structure), it is expected that the evaluation of a unique and reliable material degradation for the micro-structure of weldment (that is not possible in the present test method using a big test specimen) will be possible through the ASP test.

## References

- Abel-Latif, A. M., Corbett, J. M., Sidney D. and Taplin, D. M. R., 1981, "Effects of Microstructural Degradation on Creep Life Prediction of 2.25Cr-1Mo Steel," *Proc. of the 5th International Conference on Fracture*, Cannes, France, Vol. 4, pp. 1613~1620.
- Baik, J. M., Kameda, J. and Buck, O., 1986, "Development of Small punch Tests for Ductile-Brittle Transition Temperature Measurement of Temper Embrittled Ni-Cr Steels," *ASTM STP 888*, pp. 92~111.
- Chung, S. H., Takahashi, H. and Suzuki, M., 1978, "Microstructural Gradient in HAZ and its Influence upon Toe HAZ Fracture Toughness," *Welding in the World*, p. 248.
- Haggag, F. M., Byun, T. S., Hong, J. H., Miraglia, P. Q. and Murty, K. L., 1998, "Indentation-Energy-To-Fracture (IEF) Parameter for Characterization of DBTT in Carbon Steels Using Nondestructive Automated Ball Indentation (ABI) Technique," *Scripta Materialia*, Vol. 38, No. 4, pp. 645~651.
- Kim, J. K., Yoon, T. Y., Song, K. W., Lee, J. J. and Chung, S. H., 1991, "A Study of Evaluation for In-Service Material Degradation of High Temperature Structural Components by Grain Boundary Etching Method," *Transactions of the KSME A*, Vol. 15, No. 3, pp. 898~906.
- Lee, D. H., Lee, S. I., Kwon, I. H., Baek, S. S. and Yu, H. S., 2002, "Fracture Strength Evaluation of Heat Resisting Steel Weldment by Advanced Small Punch Test," *Proc. KWS Welding Strength Research Workshop*, pp. 76~83.
- Liao, J., Ikeuchi, K. and Matsuda, F., 1998, "Toughness Investigation on simulated weld HAZs of SQV-2A Pressure Vessel Steel," *Nuclear Engineering and Design*, Vol. 183, pp. 9~20.
- Lyu, D. Y., Chung, S. H., Lim, J. K., Jung, H. D., Tamakawa, K. and Takahashi, H., 1989, "A Study on Fracture Strength Evaluation of Steel Welded Joint by Small Punch Test (I)," *Journal of KWS*, Vol. 7, No. 3, pp. 28~35.
- Nishiyama, Y., Fukuya, K., Suzuki, M. and Eto, M., 1998, "Irradiation Embrittlement of  $2\frac{1}{4}$ Cr-1Mo Steel at 400°C and its Electrochemical Evaluation," *Journal of Nuclear Materials*, 258-263, pp. 1187~1192.
- Viswanathan, R., 1993, "Damage Mechanisms and Life Assessment of High Temperature Components," *ASM International Metals Park*, pp. 206~208.
- Yu, H. S., Ahn, B. G., Lyu, D. Y. and Chung, S. H., 1998, "A Study on Fracture Toughness of Welded Joint and Orientation in TMCP Steel by the SP Test," *Journal of KWS*, Vol. 16, No. 6, pp. 35~43.